

First-principles study of phase stability and electronic properties of RhZr

HU Jie-qiong, PAN Yong, XIE Ming

State Key Laboratory of Advanced Technologies for Comprehensive Utilization of Platinum Metals,
Kunming Institute of Precious Metals, Kunming 650106, China

Received 25 September 2010; accepted 1 March 2011

Abstract: First-principles calculations were carried out to investigate the structural stabilities and electronic properties of RhZr. The plane wave based pseudopotential method was used, in which both the local density approximation (LDA) and the generalized gradient approximation (GGA) implanted in the CASTEP code were employed. The internal positions of atoms in the unit cell were optimized and the ground state properties such as lattice parameter, density of state, cohesive energies and enthalpies of formation of ortho-RhZr and cubic-RhZr were calculated. The calculation results indicate that ortho-RhZr can form more easily than cubic-RhZr and the ortho-RhZr is more stable than cubic-RhZr. The density of states (DOS) reveals that the strong bonding in the Rh–Zr and Rh–Rh or Zr–Zr interaction chains accounts for the structural stability of ortho-RhZr and the hybridization between Rh-4d states and Zr-4d states is strong.

Key words: RhZr; first-principles; phase stability; electronic properties

1 Introduction

In the past decades, the platinum metal alloys such as the iridium alloy and rhodium alloy [1–3], have attracted much attention for their exceptional properties, such as high-temperature resistance, high-temperature oxidation resistance and high strength. Rhodium alloy has gained a wider application than iridium alloy in various fields for the better high-temperature oxidation resistance and thermoelectric properties.

Rh–Zr system is well known for its superconducting phases [4–6]. MATTHIAS [7] discovered that the superconductivity in the Rh–Zr system constitutes the first cast of numerous investigations. ZEGLER [8] produced a tentative phase diagram of the Zr-rich field and discovered the metastable omega phase. EREMENKO et al [9] suggested the Rh-rich field of Rh–Zr in a brief study of transition metals systems involving Zr. TOGANO and TACHIKAWA [10] succeeded the amorphization of alloys containing approximately 25% Rh in mole fraction. Despite those efforts, in the Rh–Zr system, RhZr intermetallic compound has been the subject of a few theoretical and

experimental works [11–12]. The high temperature structure of RhZr is of the CsCl type according to the results of RAMAN and SCHUBERT [13] and EREMENKO et al [14]. At 923 K the equiatomic RhZr undergoes a martensitic transformation. The low temperature modification of RhZr has presumably an orthorhombic symmetry, FeB-type structure [11]. Many properties (including phase stabilities, as well as electronic properties) of RhZr intermetallic compound still need to be understood at an atomic level. Here, we performed first principles calculations to investigate the phase stability and electronic properties for RhZr.

2 Crystal structure and calculation details

The B2 structure of RhZr is a cubic structure containing two atoms in the primitive unit cell. It belongs to the space group *Pm-3m*-number 221 and Pearson symbol *cP2*. The Wyckoff positions of the atoms are Rh (0, 0, 0) and Zr (1/2, 1/2, 1/2) [15]. The crystal structure of cubic-RhZr is presented in Fig. 1(a). The B27 structure is orthorhombic structure containing eight atoms in the primitive unit cell. It belongs to the space group *Pnma*-number 62 and Pearson symbol *oP8*. The

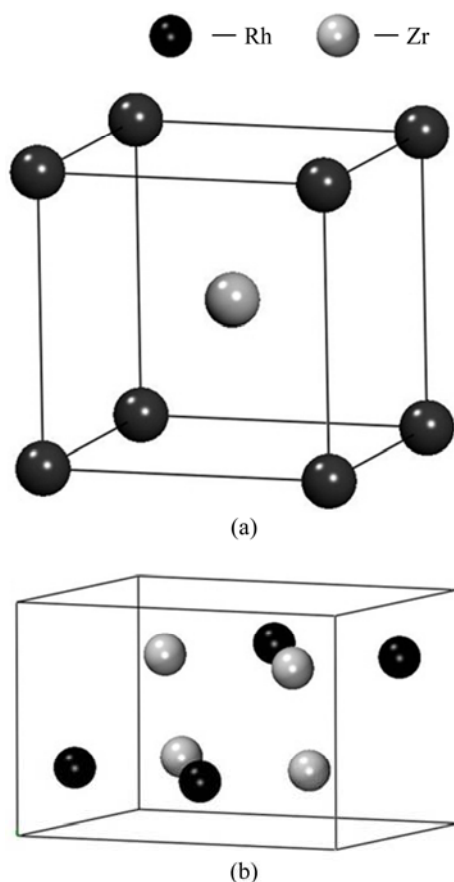


Fig. 1 Models of RhZr compound: (a) Crystal structure of cubic-RhZr (CsCl type); (b) Crystal structure of ortho-RhZr (FeB type)

atom positions of ortho-RhZr are Rh (0.032, 0.25, 0.61) and Zr (0.18, 0.25, 0.12) [6]. The crystal structure of ortho-RhZr is shown in Fig. 1(b).

All calculations are performed with Cambridge serial total energy package (CASTEP) code based on the first-principles method within the framework of density function theory (DFT) [16–17]. Vanderbilt-type ultrasoft pseudopotentials (USPP) [18] are employed to describe the electron-ion interactions. The exchange and correlation terms are described with the local-density approximation (LDA) [19] parameterized by PERDEW

and ZUNGER [20] and generalized gradient approximation (GGA) in the scheme of Perdew-Wang 91 (PW91) [21]. It needs to be mentioned that the used USPP should be compatible with the special type of LDA and GGA. For the Brillouin-zone sampling, the Monkhorst-pack scheme [22] is adopted.

In the calculations of cubic-RhZr, we use $8 \times 8 \times 8$ mesh of special k -points and the kinetic energy cutoff (E_{cut}) of 320 eV for the LDA calculations, and $E_{\text{cut}}=320$ eV, (888) k -mesh for the GGA calculations. In the calculations of ortho-RhZr, we use $6 \times 7 \times 6$ mesh of special k -points and the kinetic energy cutoff (E_{cut}) of 320 eV for the LDA calculations, and $E_{\text{cut}}=320$ eV, (676) k -mesh for the GGA calculations.

3 Results and discussion

3.1 Structural and energetic stability of phases

The ground state properties of cubic-RhZr and ortho-RhZr are investigated from their total energy, which is calculated as a function of volume. When it accords to the Murnaghan equation of state [23], the equilibrium lattice constant can be obtained (Table 1). It can be found that the GGA values of the lattice constants match fairly well with the experimental ones for cubic-RhZr (the error less than 1%). The error of LDA is larger than that of GGA. For the ortho-RhZr, the calculated lattice parameters of a and c within LDA are larger than the experimental values by 9% and 3%, respectively, while the GGA values are larger by 6% and 2%. The GGA values of a and c are as the equilibrium lattice constants of the optimized structure. LDA values are as references for a subsequent calculation.

The calculated cohesive energies and enthalpies of formation are presented in Table 1. The cohesive energy (E_c) of RhZr is calculated using formula (1) [24–25]:

$$E_c = -E_{\text{tot}}^{\text{RhZr}} + E^{\text{Rh}_{\text{atom}}} + E^{\text{Zr}_{\text{atom}}} \quad (1)$$

where $E_{\text{tot}}^{\text{RhZr}}$ is the total energy of RhZr; $E^{\text{Rh}_{\text{atom}}}$ and $E^{\text{Zr}_{\text{atom}}}$ represent the energy of the free atoms.

Table 1 Experimental and calculated lattice constants (a , b , c), cohesive energies (E_c) and formation enthalpies (ΔH_f) of cubic-RhZr (CsCl type) and ortho-RhZr (FeB type)

Structure	Method	Group	$a/\text{\AA}$	$b/\text{\AA}$	$c/\text{\AA}$	E_c/eV	$\Delta H_f/\text{eV}$
RhZr(CsCl)	LDA	Pm-3m	3.234	3.234	3.234	9.226	-8.679
	GGA		3.284	3.284	3.284	8.868	-10.785
	Exp. [15]		3.295	3.295	3.295		
RhZr(FeB)	LDA	Pnma	6.036	4.407	5.206	9.312	-8.765
	GGA		6.213	4.450	5.266	8.974	-10.892
	Exp. [6]		6.630	4.410	5.380		

The enthalpy of formation (ΔH_f^{RhZr}) is calculated according to the formula (2) [25]:

$$\Delta H_f^{\text{RhZr}} = E_{\text{tot}}^{\text{RhZr}} - E^{\text{Rh}_c} - E^{\text{Zr}_c} \quad (2)$$

where E^{Rh_c} and E^{Zr_c} are the total energies of the most stable ground state structures of the corresponding elemental metals.

It can be seen from Table 1 that the calculated cohesive energies of ortho-RhZr are higher than those of cubic-RhZr within both LDA and GGA, which shows that ortho-RhZr is more stable than cubic-RhZr at ambient condition. We believe that cubic-RhZr may transform to the more stable ortho-RhZr under certain condition, which accords with the experimental observation. The enthalpies of formation of cubic-RhZr and ortho-RhZr cell are all negative, which means that the structures of these compounds can exist and are thermodynamically stable [6, 26–27]. Cubic-RhZr cell shows a higher value of the formation enthalpy than the ortho-RhZr cell, which indicates that RhZr with orthorhombic structure is formed more easily than cubic-RhZr.

3.2 Electronic properties

Almost all the macroscopical properties of materials, such as hardness, elasticity, and conductivity, originate from their electronic structure properties as well as the nature of the chemical bonding. Therefore, it is necessary to perform the electronic structure analysis of RhZr. In this part, two parameters are used to indicate the electronic structures and chemical bonding characteristics of all RhZr phases, namely, density of states (DOS) and electron charge density difference distribution.

3.2.1 Density of states

The DOS is an important quantity for understanding the bonding in a compound. After geometry optimization, the total and partial DOS at equilibrium lattice constants for cubic-RhZr and ortho-RhZr cells are calculated, as shown in Fig. 2. In Fig. 2 it is shown that the total DOS is mainly constituted by the rhodium 4p and 4d and zirconium 4p and 4d states. For the cubic-RhZr structure the DOS can be divided into three main regions: 1) from -5 to -1.2 eV with strongly hybridizing rhodium 4d states and zirconium 4d states; 2) -1.2 to 10 eV with mainly zirconium 4d states and a lesser degree of hybridizing rhodium 4d states; 3) 10 to 20 eV with rhodium 4p states and a lesser degree of hybridizing zirconium 4p states. For the ortho-RhZr structure the DOS can be divided into two main regions: 1) from -5 to -0.8 eV with strongly hybridizing rhodium 4d states and zirconium 4d states; 2) -0.8 to 4 eV with mainly zirconium 4d states and a lesser degree of hybridizing

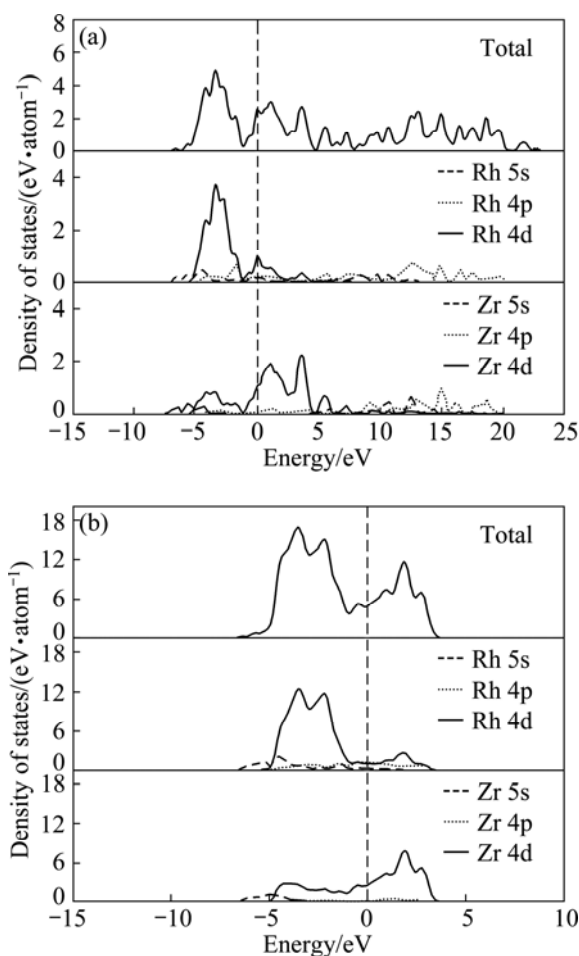


Fig. 2 Calculated total and partial density of states for RhZr in cubic-RhZr (CsCl type) (a) and ortho-RhZr (FeB type) (b) (The vertical dotted line at zero indicates the Fermi level)

rhodium 4d states. Therefore, most of the bonding for the two structures is constituted by the strong hybridization between rhodium 4d states and zirconium 4d states. Furthermore, the bandwidth (about 4.2 eV) of the filled Rh-4d bands in ortho-RhZr (Fig. 2(b)) is wider than that of cubic-RhZr (about 3.8 eV) (Fig. 2(a)), the increased Rh d-band width from ortho-RhZr to cubic-RhZr is due to the increased Rh–Rh interactions in ortho-RhZr, which is in good agreement with the calculated result.

It can also be seen from Fig. 2 that the calculated DOS of cubic-RhZr and ortho-RhZr presents a well defined low-energy bonding and high-energy anti-bonding region. A deep valley separates the bonding and anti-bonding sections of the DOS. Obviously, the phase stability of the compounds depends on the number of valence electrons participating in bonding below the Fermi level. For ortho-RhZr, as shown in Fig. 2(b), the number of valence electrons participating in bonding is larger than that of cubic-RhZr (Fig. 2(a)), which indicates that RhZr with orthorhombic structure is more stable than cubic-RhZr.

3.2.2 Electron charge density difference distribution

In order to gain more insight into the bonding nature of ground state RhZr, we also investigate the electron charge density maps. The electron charge density difference distributions of two structures of RhZr on the different plane are shown in Fig. 3. The contour lines are plotted from $-0.411\ 0$ to $0.100\ 5\ e/\text{\AA}^3$.

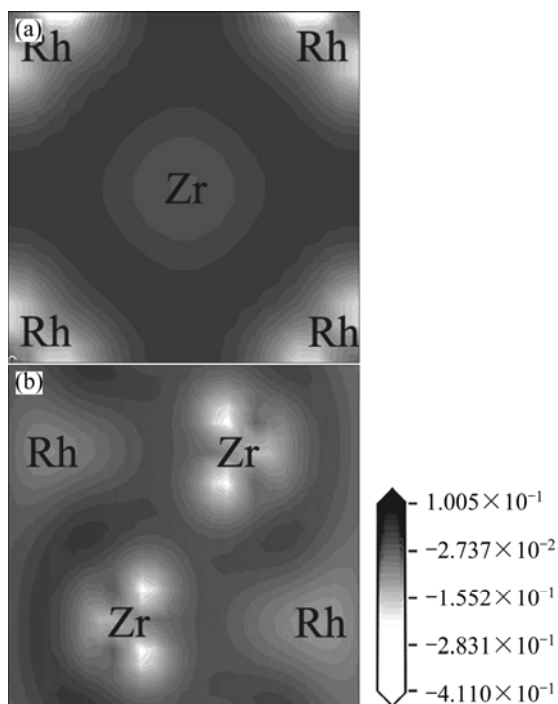


Fig. 3 Electron density difference in cubic-RhZr (0 0 1) plane (a) and ortho-RhZr (FeB-type) (1 0 0) plane (b) (The bonding charge density ranges from $-0.411\ 0\ e/\text{\AA}^3$ (depleted region: white) to $0.100\ 5\ e/\text{\AA}^3$ (enhanced region: black). The contour lines are drawn at a constant interval.)

The electron charge density difference is defined as the charge density difference between RhZr and the superposition of atomic charge densities, i.e. [28],

$$\Delta\rho(\mathbf{r}) = \rho(\mathbf{r}) - \sum_{\mu} \rho_{\text{atom}}(\mathbf{r} - \mathbf{R}_{\mu}) \quad (3)$$

where $\rho_{\text{atom}}(\mathbf{r} - \mathbf{R}_{\mu})$ is the atomic charge density. Such a map can help to visualize the characteristic of bonding. In Fig.3, the charge accumulation (black) and depletion (white) regions relative to the non-interacting atoms are clearly shown. From Fig. 3 (a), strong covalent occurs, i.e., significantly directional charge accumulation between the atoms. In the same way, the interacting bond between Rh and Zr atoms mixed with Zr–Zr interaction chains in the ortho-RhZr can be seen in Fig. 3(b). The charge redistribution plots illustrate that the interactions in ortho-RhZr is stronger than that in cubic-RhZr, and the strong bonding in the Rh–Zr and Rh–Rh or Zr–Zr interaction chains accounts for the structural stability of

ortho-RhZr. The structural stability implies that ortho-RhZr tends to maintain its orthorhombic structure in experiment if there is no strong external influence. The destabilization of cubic-RhZr may be due to lack of Rh–Rh or Zr–Zr interaction chains, which leads to the change of the shortage of bonding formed in cubic-RhZr.

4 Conclusions

1) The calculated equilibrium structural parameters of cubic-RhZr and ortho-RhZr are close to the experimental results. The calculated formation enthalpy and cohesive energies values indicate that cubic-RhZr and ortho-RhZr are thermodynamically stable. Cubic-RhZr cell shows a higher value of the formation enthalpies than the ortho-RhZr cell, which indicates that RhZr with orthorhombic structure is formed more easily than cubic-RhZr. It is also confirmed that ortho-RhZr is more stable than cubic-RhZr at ambient condition from the calculated cohesive energies of cubic-RhZr and ortho-RhZr.

2) The calculated DOS of cubic-RhZr and ortho-RhZr notes that the total DOS is mainly constituted by the rhodium 4p and 4d and zirconium 4p and 4d states, and the most of the bonding for the two structures is constituted by the strong hybridization between the rhodium 4d states and zirconium 4d states. Furthermore, the number of valence electrons participating in bonding of ortho-RhZr is larger than that of cubic-RhZr, which indicates that RhZr with orthorhombic structure is more stable than cubic-RhZr.

3) From the electron density difference distribution results, it is found that the interactions in ortho-RhZr is stronger than cubic-RhZr, and the strong bonding in the Rh–Zr and Rh–Rh or Zr–Zr interaction chains accounts for the structural stability of ortho-RhZr.

References

- [1] YAMABE Y, KOIZUMI Y, MURAKAMI H. Development of Ir-base refractory superalloys [J]. Scripta Materialia, 1996, 35(2): 211–215.
- [2] YAMABE Y, KOIZUMI Y, MURAKAMI H. Rh-base refractory superalloys for ultra-high temperature use [J]. Scripta Materialia, 1997, 36(4): 393–398.
- [3] MIURA S, HONMA K, SANCHEZ J M. Mechanical properties of Rh-based L_{12} intermetallic compounds Rh_3Ti , Rh_3Nb and Rh_3Ta [J]. Intermetallics, 2000, 8(7): 785–791.
- [4] MASSALSKI T B. Binary alloy phase diagrams [M]. Metals Park, OH: ASM International, 1992.
- [5] VILLARS P, CENZUAL K, HULLIGER F, MASSALSKI T B, OKAMOTO H, OSAKI K. Inorganic materials database and design system [M]. Metals Park, OH: ASM International, 2003.
- [6] JORDA J L, GRAF T, SCHELLENBERG L, MULLER J. Phase relations, thermochemistry and superconductivity in the Zr-Rh system [J]. J Alloy Compd, 1988, 136(2): 313–328.
- [7] MATTHIAS B T. The superconductivity in Rh-Zr system [J]. Phys Rev Lett, 1955, 97: 74–76.

- [8] ZEGLER S T. Superconductivity in zirconium-rhodium alloys [J]. Phys Chem Solids, 1964, 26(8): 1347–1349.
- [9] EREMENKO V M, SEMENOVA E L, SHMENA T D. Study of transition metals systems involving Zr suggested the Rh-rich field of Rh-Zr [J]. Metallofiz Nov Tekh, 1974, 52: 112–115.
- [10] TOGANO K, TACHIKAWA K. Upper critical fields and critical currents of superconducting zirconium-rhodium alloys [J]. J Less-Common Met, 1973, 33(2): 275–282.
- [11] JORDA J L, GACHON J C, CHARLES J, HERTZ J. High temperature study of the zirconium- rhodium system [J]. Journal of Thermal Analysis, 1988, 34: 551–557.
- [12] GUO Q T, KLEPPA O J. Standard enthalpies of formation of some alloys formed between group IV elements and group VIII elements, determined by high-temperature direct synthesis calorimetry I: Alloys of (Ti, Zr, Hf) with (Rh, Pd, Pt) [J]. J Alloy Compd, 1998, 266(1): 224–229.
- [13] RAMAN A, SCHUBERT K. The high temperature structure in Zr-Rh system [J]. Z Metallkunde, 1964, 55: 704–706.
- [14] EREMENKO V N, SEMENOVA E L, SHMENA T D, KUDRYAVTSEV V. Phase relations and structures in zirconium-rhodium alloys [J]. Dopovidi Akad Nauk A, 1978, 10: 943–947.
- [15] SEMENOVA E L, KUDRYAVTSEV Y V. Structural phase transformation and shape memory effect in ZrRh and ZrIr [J]. J Alloy Compd, 1994, 203(4): 165–168.
- [16] KOHN W, SHAM L J. Self-consistent equations including exchange and correlation effects [J]. Phys Rev A, 1965, 140(4): 1133–1138.
- [17] HOHENBERG P, KOHN W. Inhomogeneous electron gas [J]. Phys Rev B, 1964, 136(3): 864–871.
- [18] VANDERBILT D. Soft self-consistent pseudopotentials in generalized eigenvalue formalism [J]. Phys Rev B, 1990, 41(11): 7892–7895.
- [19] CEPERLEY D M, ALDER B J. Ground state of the electron gas by a stochastic method [J]. Phys Rev Lett, 1980, 45(7): 566–569.
- [20] PERDEW J P, ZUNGER A. Self-interaction correction to density-functional approximations for many-electron systems [J]. Phys Rev B, 1981, 23(10): 5048–5079.
- [21] PERDEW J P, CHEVARY J A, VOSKO S H, JACKSON K A, FIOUHAIS C. Atoms, molecules, solids, and surfaces: Applications of the generalized gradient approximation for exchange and correlation [J]. Phys Rev B, 1992, 46(11): 6671–6687.
- [22] MONKHORST H J, PACK J D. Special points for Brillouin-zone integrations [J]. Phys Rev B, 1976, 13(12): 5188–5192.
- [23] MURNAGHAN F D. The compressibility of media under extreme pressures [J]. PNAS, 1944, 30(9): 244–247.
- [24] KELLOU A, FARAOUN H I, GROSSEIDIER T, CODDET C, AOURAG H. Energetics and electronic properties of vacancies, anti-sites, and atomic defects (B, C, and N) in B2-FeAl alloys [J]. Acta Mater, 2004, 52(11): 3263–3271.
- [25] STOJKOVIC M, KOTESKI V, CEKIC B, STOJIC D, IVANOVSKI V. Structure and electronic properties of Mo₃Pt, MoPt₂, and MoPt₃: First-principles calculations [J]. Phys Rev B, 2008, 77(19): 193111.
- [26] TOPOR L, KLEPPA O J. Standard enthalpies of formation of RhTi, RhZr and RhHf [J]. J Alloy Compd, 1987, 135(1): 67–75.
- [27] CURTAROLO S, MORGAN D, CEDER G. Accuracy of ab initio methods in predicting the crystal structures of metals: A review of 80 binary alloys [J]. Calphad, 2005, 29: 163–211.
- [28] HU C H, YANG Y, ZHU Z Z. Structural stability and electronic properties of LiNiN [J]. Solid State Communications, 2010, 150: 669–674.

RhZr 相结构稳定性和电子结构性质的第一性原理研究

胡洁琼, 潘勇, 谢明

昆明贵金属研究所 稀贵金属综合利用新技术国家重点实验室, 昆明 650106

摘要: 用第一性原理计算研究 RhZr 两种晶体结构的结构稳定性和电子结构性质。采用基于第一性原理的平面波赝势法, 分别用局域密度近似和广义梯度近似法, 对晶体原子的结构进行优化, 并分别对正交晶系 RhZr 和立方晶系 RhZr 的基态性质, 如晶格参数、能态密度、形成能以及形成焓等进行计算。计算结果表明: 正交晶系 RhZr 比立方晶系 RhZr 更容易生成, 而且生成的正交晶系 RhZr 比立方晶系 RhZr 更稳定。能态密度计算结果表明: 立方晶系 RhZr 比正交晶系 RhZr 稳定, 是因为在立方晶系 RhZr 中不仅存在 Rh-Zr 还存在 Rh-Rh 或者 Zr-Zr 之间的相互作用键。由态密度分析还可看出, 在费米面附近 Rh 的 4d 轨道与 Zr 的 4d 轨道存在较强的轨道杂化。

关键词: RhZr; 第一性原理; 相结构稳定性; 电子结构性质

(Edited by YANG Hua)